

Learning the Distribution: A Unified Distillation Paradigm for Fast Uncertainty Estimation in Computer Vision

Yichen Shen^{*}
Samsung Inc, USA

Zhilu Zhang^{*}
Cornell University

Mert R. Sabuncu
Cornell University

Lin Sun
Samsung Inc, USA

Abstract

Calibrated estimates of uncertainty are critical for many real-world computer vision applications of deep learning. While there are several widely-used uncertainty estimation methods, dropout inference [11] stands out for its simplicity and efficacy. This technique, however, requires multiple forward passes through the network during inference and therefore can be too resource-intensive to be deployed in real-time applications. To tackle this issue, we propose a unified distillation paradigm for learning the conditional predictive distribution of a pre-trained dropout model for fast uncertainty estimation of both aleatoric and epistemic uncertainty at the same time. We empirically test the effectiveness of the proposed method on both semantic segmentation and depth estimation tasks, and observe that the student model can well approximate the probability distribution generated by the teacher model, i.e the pre-trained dropout model. In addition to a significant boost in speed, we demonstrate the quality of uncertainty estimates and the overall predictive performance can also be improved with the proposed method.

1. Introduction

Uncertainty exists in many machine learning problems due to noise in the observations and incomplete coverage of domain. How certain can we trust the model built upon limited yet imperfect data? Reliable uncertainty estimates are crucial for trustworthy applications such as medical diagnosis and autonomous driving. Many algorithms have been proposed to estimate the uncertainty of neural networks (NN) [3, 23, 26, 37]. Among these, the MC dropout [11] is arguably one of the most popular approaches due to its simplicity and scalability. [22] further explored the idea of incorporating both aleatoric and epistemic uncertainty into deep neural networks in computer vision based on MC Dropout. This approach has been adopted in different computer vision tasks recently tasks [1, 10].

^{*}equal contribution

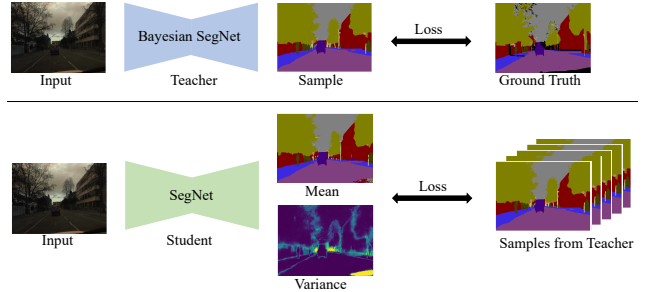


Figure 1: An illustration of the proposed method. Given a trained teacher, a deterministic student is used to approximately parameterize the predictive distribution of the teacher model, thereby achieving sample-free uncertainty estimates.

Despite its successful demonstration in various computer vision tasks [22], MC dropout requires test-time sampling to obtain uncertainty. This costly sampling process can introduce severe latency in real-time prediction tasks such as the perception system of self-driving vehicles and leads to undesired consequences.

Inspired by the recent success of knowledge distillation [17], prior work [5] has explored the idea of distilling the knowledge from MC dropout samples from a teacher model into a student network (Dropout Distillation or DD) in order to eliminate the expensive dropout sampling at the test-time. Nevertheless, DD has several limitations. Specifically, the student model only learns from the predictive means of the dropout teacher model. As such, the dispersion of the teacher’s prediction, which entails important uncertainty information associated with the predictions [31], is completely neglected in their approach. In addition, in the context of regression tasks, no uncertainty information can be obtained from the student network. These limitations not only lead to sub-optimal student performance, but also severely limit its applicability in computer vision tasks, where most of the problems consist of both regression and classification.

Contributions. In this paper, we propose a novel knowl-

edge distillation framework to directly approximate the predictive distribution produced by a dropout teacher with a parametric distribution instead of learning only the mean prediction of the teacher. At test time, the parameters of the distribution are output by a single deterministic student network to obtain reliable uncertainty estimates. To further enhance the richness of uncertainty estimates, we propose to incorporate both epistemic and aleatoric uncertainty into our distillation framework with little extra computation.

We empirically examine the effectiveness of the proposed method on both regression and classification tasks. For regression, we experiment on monocular depth estimation using NYU DepthV2 [33] and KITTI [14]. For classification, we experiment on semantic segmentation using CamVid [4] and VOC2012 [9]. Quantitative and qualitative results show the student network produces uncertainty estimates of better quality than those of the teacher model, i.e. MC dropout pre-trained model. We also show that the predictive mean and uncertainty obtained with our method are superior to those learned from DD proposed by [5].

Although our derivations are done with respect to the MC dropout, the proposed method can be easily extended to any other forms of sampling-based uncertainty estimation algorithms. In particular, we demonstrate our method can capture both epistemic and aleatoric uncertainty from deep ensembles [25].

2. Related Work

Uncertainty estimation can be obtained for deep learning in a principled manner through Bayesian neural networks [28, 34]. However, they typically suffer from significant computational burdens due to the intractability of posteriors. As such, computational tractability has been a primary focus of research. One such direction is through Markov Chain Monte Carlo (MCMC) [34]. For instance, stochastic gradient versions of MCMC have been proposed [7, 15, 27, 36] to scale MCMC method to large datasets. Nevertheless, these approaches can be difficult to scale to high-dimensional data. An alternative solution is through variational inference in which parametric distributions are used to approximate the intractable true posteriors of the weights of neural networks [3, 23, 26, 37]. However, the variational inference can suffer from sub-optimal performances [2].

There have also been Non-Bayesian techniques for uncertainty estimation. For instance, an ensemble of randomly-initialized NNs [25] has shown to be effective. Nevertheless, they require training and saving multiple NNs, which can be resource inefficient. Methods to more efficiently obtaining ensembles exist [13, 18], but these can come at the cost of quality of uncertainty estimates.

Most of the above-mentioned methods require multiple forward passes of NNs at test time, which prohibits their deployment in real-time computer vision systems. Several

techniques have been proposed to speed up uncertainty estimation. Postels et al. [35] proposed a method for sampling-free uncertainty estimation through variance propagation. However, the technique makes several simplistic assumptions about the covariance matrices of NNs, which can lead to inaccurate approximations. Another approach speeds up the sampling process by leveraging the temporal information in videos [19]. However, the method cannot be generically applied and results in a non-trivial drop in predictive performance. Ilg et al. [20] proposed the use of a multi-hypotheses NN with a novel loss function to obtain sample-free uncertainty estimates. Nevertheless, it can lead to hypothesis collapse thereby underestimating uncertainty.

Distillation-based methods have also been explored. [5] proposed to distill predictive means from a dropout teacher to a student network. As mentioned above, this setup leads to the loss of the epistemic uncertainty of the MC dropout teacher. [32] proposed a similar distillation approach from an ensemble of networks. However, this approach fails to account for aleatoric uncertainty. Moreover, no prior work has demonstrated the effectiveness of distillation for fast uncertainty estimation in a scalable way beyond toy datasets. In this work, we aim to fill this gap.

3. Method

Suppose we have a dataset $\mathcal{D} = (\mathbf{X}, \mathbf{Y}) = \{(\mathbf{x}_i, \mathbf{y}_i)\}_{i=1}^n$, where each $(\mathbf{x}_i, \mathbf{y}_i) \in (\mathcal{X} \times \mathcal{Y})$ is i.i.d. and $\mathcal{X} \subseteq \mathbb{R}^d$ corresponds to the feature space. Most tasks in computer vision can be considered as either regression or classification. For regression, $\mathcal{Y} \subseteq \mathbb{R}^k$ for some integer k , and in the context of k -class classification, $\mathcal{Y} = \{1, \dots, k\}$ is the label space. We define $f_{\mathbf{w}}(\mathbf{x})$ to be a neural network such that $f : \mathcal{X} \rightarrow \mathcal{Y}$, and $\mathbf{w} = \{W_i\}_{i=1}^L$ corresponds to the parameters of the network with L -layers, where each W_i is the weight matrix in the i -th layer. We define the model likelihood $p(\mathbf{y}|\mathbf{x}, \mathbf{w}) = p(\mathbf{y}|f_{\mathbf{w}}(\mathbf{x}))$. For regression tasks, it is common to assume $p(\mathbf{y}|f_{\mathbf{w}}(\mathbf{x})) = \mathcal{N}(f_{\mathbf{w}}(\mathbf{x}), \sigma^2)$, for some noise term σ . For classification tasks, $p(\mathbf{y}|f_{\mathbf{w}}(\mathbf{x})) = \text{Softmax}(f_{\mathbf{w}}(\mathbf{x}))$ is commonly assumed. To capture epistemic uncertainty, we put a prior distribution on the weights of the network, $p(\mathbf{w})$. A common choice is the zero mean Gaussian $\mathcal{N}(0, I)$. Bayes Theorem can then be used to obtain the posterior $p(\mathbf{w}|\mathbf{X}, \mathbf{Y}) = p(\mathbf{Y}|\mathbf{X}, \mathbf{w})p(\mathbf{w})/p(\mathbf{Y}|\mathbf{X})$, with which the predictive distribution can be determined by

$$p(\mathbf{y}|\mathbf{x}, \mathcal{D}_{\text{train}}) = \int p(\mathbf{y}|\mathbf{x}, \mathbf{w})p(\mathbf{w}|\mathcal{D}_{\text{train}})d\mathbf{w}. \quad (1)$$

3.1. Preliminary: Dropout for Bayesian Deep Learning

The marginal distribution $p(\mathbf{Y}|\mathbf{X})$, and thus $p(\mathbf{w}|\mathbf{X}, \mathbf{Y})$ are often intractable. Variational inference uses a tractable family of distributions $q_{\theta}(\mathbf{w})$

parameterized by θ to approximate the true posterior $p(\mathbf{w}|\mathbf{X}, \mathbf{Y})$, thereby turning the intractable problem into a tractable optimization task. MC dropout, which casts the commonly used dropout regularization as approximate Bayesian inference, is one such example [11]. It involves training NNs with dropout after each weight layer. With an optimized model, the approximate predictive distribution is given by $q(\mathbf{y}|\mathbf{x}, \mathcal{D}_{\text{train}}) = \int p(\mathbf{y}|\mathbf{x}, \mathbf{w})q_\theta(\mathbf{w})d\mathbf{w}$. The integral can be approximated through performing Monte Carlo integration over the approximate distribution $q_\theta(\mathbf{w})$. This corresponds to dropout at test time. In classification for example,

$$p(y = c|\mathbf{x}, \mathcal{D}_{\text{train}}) \approx \frac{1}{T} \sum_{t=1}^T \text{Softmax}(f_{\mathbf{w}_t}(\mathbf{x})), \quad (2)$$

where $\mathbf{w}_t \sim q_\theta(\mathbf{w})$ are dropout samples from the NN.

Epistemic uncertainty can be computed with the approximate inference framework as derived above. For regression, epistemic uncertainty is captured by the predictive variance, which can be approximated by computing the variance of the dropout approximate distribution:

$$\sigma_y^2 \approx \frac{1}{T} \sum_{t=1}^T f_{\mathbf{w}_t}(\mathbf{x})^T f_{\mathbf{w}_t}(\mathbf{x}) - \mu_y^T \mu_y, \quad (3)$$

where $\mu_y = \sum_{t=1}^T f_{\mathbf{w}_t}(\mathbf{x})$. In the context of classification, numerous measures have been proposed as uncertainty estimates [12]. In this paper, we use the mutual information between the predictions and the model posterior (BALD),

$$\mathbb{I}[\mathbf{y}, \mathbf{w}|\mathbf{x}, \mathcal{D}_{\text{train}}] = \mathbb{H}[\mathbf{y}|\mathbf{x}, \mathcal{D}_{\text{train}}] - \mathbb{E}[\mathbb{H}[\mathbf{y}|\mathbf{x}, \mathbf{w}]] \quad (4)$$

as the uncertainty estimates for all our experiments in classification tasks.

As proposed by Kendall and Gal [22], aleatoric uncertainty can also be incorporated into the dropout model for concurrent estimation of both the epistemic and aleatoric uncertainty. To do so, an input-dependent observation noise parameter $\hat{\sigma}^2$ is output together with the prediction

$$[\hat{\mu}, \hat{\sigma}^2] = f_{\mathbf{w}}(\mathbf{x}), \quad (5)$$

where $\hat{\sigma}^2$ is a vector with the same dimension as $\hat{\mathbf{y}}$ that represents a diagonal covariance matrix. $\hat{\sigma}$ can be optimized with maximum likelihood estimation by assuming that aleatoric uncertainty follows a parametric distribution (e.g Gaussian) for regression. For classification, this Gaussian distribution is placed over the logit space. Although the epistemic and aleatoric uncertainties are not mutually exclusive, the total uncertainty can be approximated using

$$\text{Var}(\mathbf{y}) \approx \frac{1}{T} \sum_{t=1}^T \hat{\mu}_t^T \hat{\mu}_t - \mu_y^T \mu_y + \frac{1}{T} \sum_{t=1}^T \hat{\sigma}_t^2 \quad (6)$$

where $\mu_y = \sum_{t=1}^T \hat{\mu}_t$ and the first and second term in the above expression approximates the epistemic and aleatoric uncertainties respectively.

3.2. A Teacher-Student Paradigm for Sample-free Uncertainty Estimation

Despite the success of the MC dropout, inferring uncertainty at test-time often requires multiple forward passes to generate samples of prediction, limiting its application to many time-sensitive applications. In this paper, we propose to use a deterministic neural network $f_\phi(\mathbf{x})$ to parameterize a distribution $r(\mathbf{y}|\mathbf{x}, \mathcal{D}_{\text{train}})$ that approximates the predictive distribution $q(\mathbf{y}|\mathbf{x}, \mathcal{D}_{\text{train}})$ of the dropout model. Specifically, $f_\phi(\mathbf{x})$ learns to directly output the parameters of $r(\mathbf{y}|\mathbf{x}, \mathcal{D}_{\text{train}})$. When trained, $f_\phi(\mathbf{x})$ only requires one forward pass to infer both predictive mean and uncertainty from the parameterized distribution $r(\mathbf{y}|\mathbf{x}, \mathcal{D}_{\text{train}})$, thus eliminating expensive sampling processes at test time.

Training $f_\phi(\mathbf{x})$ is straight-forward using a teacher-student paradigm similar to the knowledge distillation [17]. We first train a Bayesian neural network (BNN) $f_{\mathbf{w}}(\mathbf{x})$ (e.g. a dropout model) on $\mathcal{D}_{\text{train}}$. We then generate samples of predictions from the pre-trained $f_{\mathbf{w}}(\mathbf{x})$. These samples serve as ‘‘observations’’ from the distribution $q(\mathbf{y}|\mathbf{x}, \mathcal{D}_{\text{train}})$ for $f_\phi(\mathbf{x})$ to learn the parameters of $r(\mathbf{y}|\mathbf{x}, \mathcal{D}_{\text{train}})$ given each input $\mathbf{x} \in \mathcal{D}_{\text{train}}$. Eventually $f_\phi(\mathbf{x})$ learns an efficient mapping from input images to the parameters of the distribution $r(\mathbf{y}|\mathbf{x}, \mathcal{D}_{\text{train}})$ that accurately approximates $q(\mathbf{y}|\mathbf{x}, \mathcal{D}_{\text{train}})$. For simplicity, in the following illustration we term the BNN $f_{\mathbf{w}}(\mathbf{x})$ as the teacher model and $f_\phi(\mathbf{x})$ as the student model.

3.2.1 Sampling from the Bayesian Teacher

As mentioned above, predictive samples $\{\hat{\mathbf{y}}_t = f_{\mathbf{w}_t}(\mathbf{x})\}_{t=1}^m$ are generated from the teacher to train the student. In the more complicated scenario where aleatoric uncertainty is modeled by teacher, we incorporate aleatoric uncertainty into each predictive sample with

$$\hat{\mathbf{y}}_t = \hat{\mu}_t + \hat{\sigma}_t \epsilon, \quad \epsilon \sim \mathcal{N}(0, I). \quad (7)$$

where $\hat{\sigma}_t$ is the aleatoric uncertainty output by the teacher given an input. In practice, $\hat{\sigma}_t$ can be noisy. To stabilize training, instead of $\hat{\sigma}_t^2$, we first compute empirical mean $\tilde{\sigma}^2 \triangleq \frac{1}{T} \sum_{t=1}^T \hat{\sigma}_t^2$, and use $\tilde{\sigma}^2$ to generate all samples $\{\hat{\mathbf{y}}_t\}_{t=1}^m$.

The larger the number of samples, the more accurate the student approximation can be to the teacher predictive distribution. However, sampling a large number of samples requires intensive computational resources. To cope with this challenge, we generate a small number of m predictive samples from the teacher for each input on-the-fly at each epoch during training. In order to learn aleatoric uncertainty, we

further get k random samples from $\mathcal{N}(0, I)$ for each predictive sample $[\hat{\mu}_t, \hat{\sigma}^2]$ (see Eq. 7). In practice we use $m = 5$ and $k = 10$. As we demonstrate in the experimental section, a small number of m and k per input is sufficient to learn student model with excellent performance.

3.2.2 Optimizing the Student

We use maximum likelihood estimation (MLE) to optimize $f_\phi(x)$. Given the samples $\{\hat{y}_t\}_{t=1}^m$ generated by the teacher, we minimize the negative log likelihood for each input x

$$\mathcal{L}_{student} = - \sum_t \log r(\hat{y}_t | x; \phi). \quad (8)$$

where $r(\hat{y}_t | x; \phi)$ is parameterized by $f_\phi(x)$. In order to avoid division by zero and enable unconstrained optimization of the variance, we use log variance $s = \log(\hat{\sigma}^2)$ as the output of the student in practice. Thus, we have $[\hat{\mu}, s] = f_\phi(x)$.

For regression problems, we use the Laplace distribution to approximate the variational predictive distribution. For simplicity, we assume independence among all the dimensions of outputs so that log variance s is a vector of the same dimension as $\hat{\mu}$. Given the Laplace assumption, a numerically stable MLE training objective can be derived from Eq. 8 as

$$\mathcal{L}_{student} = \frac{1}{N} \frac{1}{M} \sum_i \sum_t \sqrt{2} \exp\left(-\frac{1}{2}s_i\right) |\hat{y}_{ti} - \hat{\mu}_i| + \frac{1}{2}s_i, \quad (9)$$

where i and t corresponds to the summation over the output space and the generated samples respectively and N and M are number of instances (e.g pixels) in the output space and the generated predictive samples from teacher, respectively. The reason to choose Laplace distribution over Gaussian distribution is because it is more appropriate to model the variances of residuals with ℓ_1 loss, which usually outperforms ℓ_2 loss in computer vision tasks.

For classification problems, we use a logit-normal distribution to model teacher’s approximate predictive distribution $q(y|x, \mathcal{D}_{train})$ on the simplex¹. In practice, we use a Gaussian distribution with a diagonal covariance matrix to approximate the teacher’s predictive distribution on the logit space. As a result, the student model outputs μ_i and s_i as the mean and log variance of the Gaussian for each member of the logits. Similar to the regression set-up, we derive a numerically stable Gaussian MLE training objective

$$\mathcal{L}_{student} = \frac{1}{N} \frac{1}{M} \sum_i \sum_t \frac{1}{2} \exp(-s_i) \|\hat{y}_{ti} - \hat{\mu}_i\|^2 + \frac{1}{2}s_i, \quad (10)$$

¹Dirichlet distribution is an obvious alternative, but we empirically observe that training with logit-normal is much more numerically stable.

where y_{ti} are predicted logits sampled from teacher. Since close-form solution does not exist for the moments of a logit-normal distribution, Monte Carlo sampling on the logit space is performed at test time to obtain uncertainty estimates. This only incurs a tiny computational overhead during inference as it amounts to multiple forward passes of one layer of the student network (the softmax function). As shown in experiments, the student model still has a large advantage in inference time over its teacher in addition to better performance.

We empirically observe that training solely with the above loss functions sometimes leads to sub-optimal predictive performance. This may be due to the noisy signal provided by the generated samples. Thus we leverage ground truth labels in addition to predictive samples from the teacher to stabilize the training of the student model. We use the loss function for which the teacher model is trained in conjunction with the $\mathcal{L}_{student}$, leading to the total loss

$$\mathcal{L}_{total} = \mathcal{L}_{student} + \lambda \mathcal{L}_{teacher}, \quad (11)$$

where the λ is a hyper-parameter to be tuned and $\mathcal{L}_{teacher}$ corresponds to the categorical cross entropy loss for classification tasks or L1 loss for regression tasks. We found that $\lambda = 1$ generally performs well for our experiments.

3.2.3 Additional Augmentation

When the same training dataset is used for both the teacher and the student training, the student may underestimate the epistemic uncertainty of the teacher due to overfitting of the teacher network to the training data. Ideally, in order to fully capture the teacher predictive distribution, the dataset used to train the student should not overlap with the one for the teacher. However, training using only a subset of available samples can lead to sub-optimal performance. To alleviate this problem, we perturb the training set during the training of the student using extra data augmentation methods unused when training the teacher, in order to synthetically generate new samples unseen by the teacher model. We choose color jittering as the augmentation method that augments each image via color jitter with random variation in the range of $[-0.2, 0.2]$ in four aspects: brightness, contrast, hue, and saturation when training the student.

As we demonstrate below, this extra augmentation during student training can be crucial for enhanced quality of uncertainty estimates. We emphasize that the additional gain in uncertainty estimates does not directly come from data augmentation, but rather from teacher predictions that more closely correspond to the test-time predictive distributions as a consequence of this augmentation. In the experiments below, we show that the teacher model does not have the same performance boost with the extra augmentation.

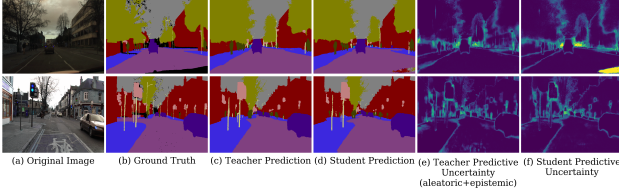


Figure 2: Example predictions on CamVid.

4. Experiments

We conduct experiments on two pixel-wise computer vision tasks: semantic segmentation and depth regression. We compare the performance of the proposed method with that of the teacher models using MC dropout. For a holistic evaluation, we consider teacher networks trained both with and without the aleatoric uncertainty. Following [22, 35], we use 50 samples for MC dropout to evaluate teacher’s performance and uncertainty. Architectures identical to that of the teacher models without the dropout layers are used as student models. As discussed in the previous section, we use 50 samples from the logit space to evaluate uncertainty (BALD) of student models for classification tasks. To demonstrate the general applicability, we also show the effectiveness of the proposed method when the teacher network corresponds to a Deep Ensemble [25].

4.0.1 Evaluation Metrics

On top of regular metrics to evaluate the performance of the predictive means of our models, we measure both the Area Under the Sparsification Error curve (AUSE) [20] and the expected calibration error (ECE) [16] as measures to evaluate the quality of uncertainty estimates. In essence, AUSE measures how much the estimated uncertainty coincides with true predictive errors. Brier score and the mean absolute error are used as predictive errors to compute AUSE for classification and regression tasks respectively. In the context of classification, ECE measures how much the predictive means of probabilities from the softmax function are representative of the true correctness of predictions. In the context of regression, we use ECE described in [24] to quantify the amount of mismatch between the predictive distribution and the empirical CDFs. We follow [24] and compute ECE with the ℓ_2 norm with a bin size of 30.

4.1. Semantic Segmentation

Bayesian SegNet [21], which contains dropout layers inserted after the central four encoder and decoder units, was proposed to obtain uncertainty estimates for semantic segmentation tasks. In this work, we use the architecture with a dropout rate of 0.5 as the teacher model for all our exper-

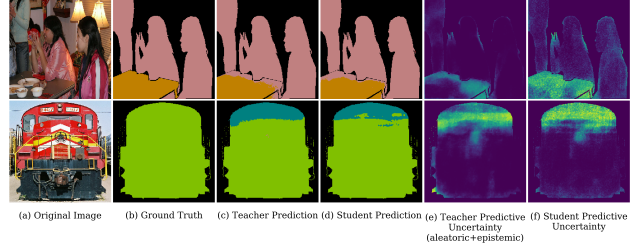


Figure 3: Example predictions on Pascal VOC2012.

iments. We evaluate the method using the CamVid and the Pascal VOC2012 datasets.

For CamVid, following Kendall et al. [21], we use 11 generalized classes and a downsampled image size of 360×480 . For the teacher network, we train using the Stochastic Gradient Descent (SGD) with an initial learning rate of 10^{-3} , a momentum of 0.9, and a weight decay of 5×10^{-4} for 100,000 steps. In order to achieve faster convergence, we initialize the student network using the weights of the teacher network. To this end, a smaller initial learning rate of 5×10^{-4} is used to train the student network for 80,000 steps. We employ a “poly” learning rate policy on both the teacher and student networks as done by Chen et al. [6]. We use a batch size of 4 for both per step.

For Pascal VOC2012, we use the same augmented “train” and “val” split as in [6]. Input images are resized to 224×224 . For the optimal performance of the teacher model, SGD with a higher initial learning rate of 10^{-2} is used instead, with a batch size of 8 for 150,000 steps. Similarly, we initialize the student model with the weights of the teacher. The student model is trained for 100,000 steps with an initial learning rate of 10^{-3} using a size of 8 per step. The performance on the “val” split is reported in the results.

Lastly, we also include the results of the student models trained using Dropout Distillation (DD) described in [5] as a comparison.

4.1.1 Evaluation

Results for both the teacher and the student are summarized in Table 1. On top of a significant boost in run-time, the student network also leads to improvements in terms of most of the metrics evaluated. We believe the reason for the observed improvements in both predictive performance and uncertainty estimates is mainly due to learning the entire predictive distribution implicitly through samples from the teacher models with the proposed optimization objective can have the *loss attenuation* effect as described in [22]. In contrast, Dropout Distribution (DD) [5], which only distills the mean prediction of the teacher as the standard knowledge distillation, shows worse performances of the student than those of the teachers in all the metrics. This further

Camvid					
Model	T	S	DD [5]	T+AU	S+AU
Accuracy \uparrow	0.906	0.907	0.903	0.907	0.909
Classwise Acc \uparrow	0.764	0.765	0.747	0.766	0.750
IOU \uparrow	0.645	0.650	0.642	0.645	0.650
ECE $\downarrow (\times 10^{-3})$	3.78	2.23	6.73	3.67	2.86
AUSE $\downarrow (\times 10^{-2})$	1.47	1.60	2.59	1.63	1.60
Runtime (s) \downarrow	1.6	0.078	0.078	2.1	0.078

Pascal VOC					
Model	T	S	DD [5]	T+AU	S+AU
Accuracy \uparrow	0.834	0.851	0.828	0.831	0.848
Classwise Acc \uparrow	0.813	0.828	0.806	0.809	0.827
IOU \uparrow	0.697	0.727	0.691	0.693	0.722
ECE $\downarrow (\times 10^{-3})$	62.7	59.0	67.5	63.0	59.0
AUSE $\downarrow (\times 10^{-2})$	4.35	3.82	4.86	4.20	4.31
Runtime (s) \downarrow	0.51	0.028	0.028	0.68	0.028

Table 1: Results on the segmentation problem. The “T”, “S” and “AU” corresponds to the teacher and student model, and the aleatoric uncertainty respectively. “T+AU” corresponds to a teacher model trained with the aleatoric uncertainty. “DD” corresponds to the student trained using Dropout Distillation [5]. Best performing results for each teacher-student pair are bold-faced.

demonstrates the benefit of distilling the entire predictive distribution from the teacher.

Figure 2 and 16 are random selected examples from the validation set of CamVid and Pascal VOC respectively. Visual examples suggest that the student model can accurately capture both the predictive mean and uncertainty of the teacher model. Furthermore, a closer comparison reveals the exceptional quality of the uncertainty estimates produced by the student model. For instance, in the first example from the CamVid dataset in Figure 2, a small part of the ego vehicle is captured by the camera at the bottom of the figure. While the teacher model confidently predicts the area as “road surface”, the student model highlights this subtle anomaly with high uncertainty estimates. A similar contrast is also observed in the top example of Figure 16, where the boundary of people is assigned much higher uncertainty by the student model. Besides, the bowls and plates on the dining table, which are not in the list of labeled classes for the dataset, also “confuses” the student model, but not the teacher.

4.1.2 Run-Time Comparison

Figure 4 (a)-(c) illustrate a comparison of running time and performance using different numbers of samples for MC dropout. While the running time of MC dropout can be shortened with fewer samples, it comes at the cost of quality of prediction and uncertainty estimates. The running time of MC Dropout is optimized by caching results before the

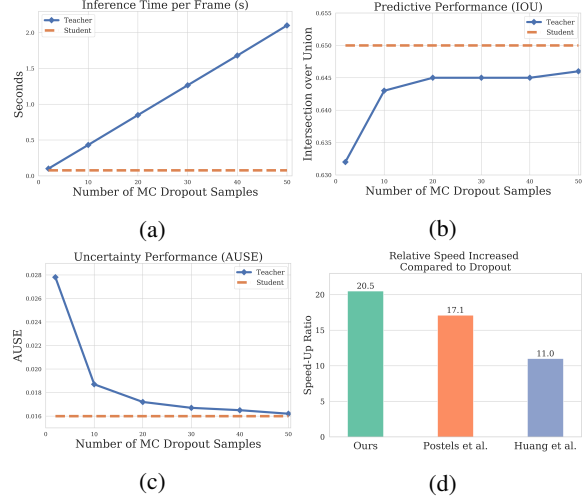


Figure 4: (a)-(c): Comparison of performance against the running time for both the teacher (with the aleatoric uncertainty) and student model using the CamVid dataset. (d) Speed-up ratios of uncertainty estimates for the CamVid dataset with the Bayesian SegNet compared to Huang et al. [19] and Postels et al. [35], two other sample-free uncertainty estimation methods.

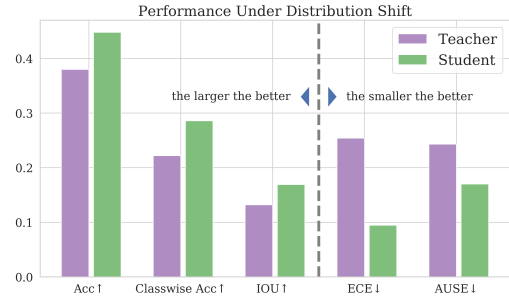


Figure 5: Performance of models trained with CamVid and evaluated on Cityscapes.

first dropout layer for a fair comparison.

We further demonstrate the merit of the proposed method by comparing the running time of the student with several other recently proposed sample-free methods for uncertainty estimates. Figure 4 (d) illustrates the speed boost with different methods on the CamVid dataset with Bayesian SegNet. The ratios are computed with respect to the same baseline of MC dropout with 50 samples at test time. Our proposed method achieves a more significant boost in speed than previously proposed methods for accelerating dropout inference, in addition to other advantages such as wider applicability and improved predictive performance.

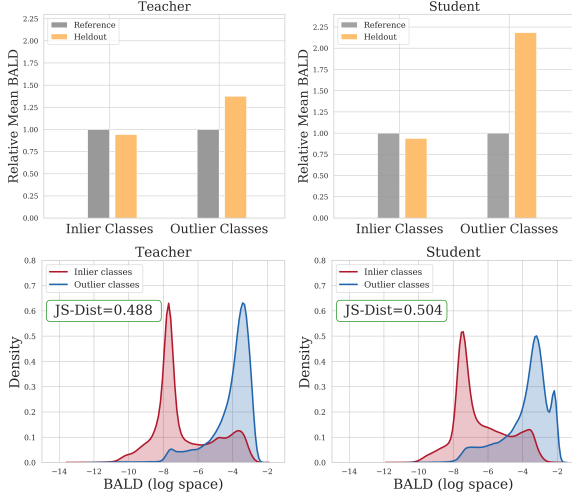


Figure 6: *Top*: Relative means of BALD for samples of seen and unseen classes during training compared to the “Reference” models, which refer to models trained with both seen and unseen classes. *Bottom*: Distribution of BALD for samples of seen and unseen classes during training.

4.1.3 Performance under Distribution Shift

We also evaluate the performance of the proposed method under a distribution shift using models trained with the CamVid dataset. The Cityscapes dataset [8], which contains street scenes collected from different cities, is an ideal dataset for such evaluation. We emphasize that neither the teacher nor the student sees images from the Cityscapes dataset during training. The results are summarized in Figure 5, which is evaluated on the overlapped classes between CamVid and Cityscapes. While both the teacher and student models perform unsatisfactorily, the student performs significantly better than the teacher in terms of all of the metrics evaluated, suggesting its enhanced robustness against the distribution shift when trained with the proposed teacher-student pipeline. This can be important for lots of application domains with long-tail scenarios like autonomous driving.

4.1.4 Outlier Detection

In addition, we examine the effectiveness of the uncertainty estimates for outlier detection using the CamVid dataset. Following [35], we use “pedestrian” and “bicyclist” as held-out classes and exclude them from training. Ideally, classes unseen during training should have much higher uncertainty estimates than that of the seen classes. We show in Figure 6 comparisons of relative means of the uncertainty estimates against those of “reference” models, which refer to models trained with both seen and unseen classes, for both inlier and outlier classes. While both teacher and stu-

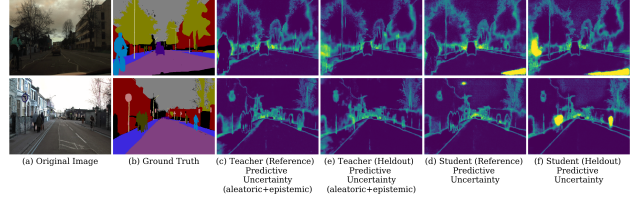


Figure 7: Example predictions on CamVid when “pedestrian” and “bicyclist” are held out during training. “Reference” refers to models trained with all classes.

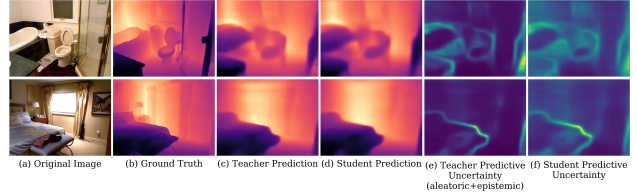


Figure 8: Example predictions on NYU V2.

dent assign higher uncertainty to outlier classes compared to the “reference” models on average, the relative mean is much higher for the student. To further quantify the performance, we also compute the JensenShannon distance between distributions of uncertainty estimates of inlier and outlier classes [29]. Again, the difference in the inlier and outlier distribution is larger for the student network, suggesting its enhanced ability for outlier detection. Lastly, we show in Figure 7 two randomly chosen examples to illustrate the difference between teacher and student. As seen clearly, regions with pedestrians and bicyclists have higher uncertainty estimates when they are not present in training for both the teacher and student. The magnitude is much larger for the student as represented by bright spots in the uncertainty plot.

4.2. Pixel-Wise Depth Estimation

For pixel-wise depth estimation tasks, NYU DEPTH V2 and the KITTI Odometry dataset are used to conduct experiments. We follow the same ResNet-based architecture to [30] for the training of both datasets in RGB based depth estimation, with dropout $p = 0.2$ placed after each convolutional layer except the final one. For NYU DEPTH V2, we use the same train/test split as in [30] and for KITTI we train our models on sequences 00-10 and evaluate them on sequences 11-21. Identical procedures are used to train the teacher models for both NYU DEPTH V2 and KITTI. During training, SGD optimizer with an initial learning rate of 0.01, a momentum of 0.9, and weight decay of 10^{-4} with “poly” learning rate poly is adopted for a total of 40 epochs. For NYU V2, we initialize the student model with the weights of the teacher and train the student model for

	NYU V2				KITTI			
Model	T	S	T+AU	S+AU	T	S	T+AU	S+AU
RMSE ↓	0.542	0.540	0.548	0.548	4.80	4.75	4.83	4.81
REL ↓	0.155	0.152	0.158	0.154	0.123	0.122	0.117	0.117
log10 ↓	0.065	0.064	0.065	0.064	0.053	0.052	0.052	0.051
$\delta 1 \uparrow$	0.793	0.798	0.794	0.799	0.843	0.847	0.845	0.846
$\delta 2 \uparrow$	0.947	0.949	0.945	0.946	0.948	0.951	0.950	0.949
$\delta 3 \uparrow$	0.985	0.984	0.982	0.981	0.981	0.982	0.981	0.981
ECE $\downarrow (\times 10^{-2})$	9.38	8.09	5.79	5.13	7.80	2.95	4.53	2.18
AUSE $\downarrow (\times 10^{-2})$	6.01	6.06	5.88	5.82	0.701	0.660	0.597	0.595
Runtime (s) ↓	0.73	0.016	0.739	0.016	0.28	0.007	0.29	0.007

Table 2: Results on the depth estimation. The “T”, “S” and “AU” corresponds to the teacher and student model, and the aleatoric uncertainty respectively. “T+AU” corresponds to a teacher model trained with the aleatoric uncertainty.

	CamVid		NYU V2	
	ECE $(\times 10^{-3})$	AUSE $(\times 10^{-2})$	ECE $(\times 10^{-3})$	AUSE $(\times 10^{-2})$
S w/o AUG	4.63	2.19	54.0	5.91
S w/ AUG	2.86	1.60	51.3	5.80
T w/o AUG	3.67	1.62	57.9	5.88
T w/ AUG	3.90	1.62	57.1	5.90

Table 3: Impact of adding augmentation in training on quality of uncertainty produced on the CamVid and NYU V2 datasets. “T” and “S” represents teacher and student models, and “AUG” corresponds to augmentation.

30 epochs using a smaller learning rate of 0.005. We empirically observe that initializing with the teacher model for KITTI leads to overfitting to the training set and thus we train the student model from scratch with the identical procedure as used for teacher training. We use a batch size of 8 in all of the depth estimation experiments.

4.2.1 Evaluation

The quantitative performance of both the teacher and the student models is summarized in Table 2. Similar to segmentation tasks, the student model outperforms the teacher in most of the evaluation metrics. Example predictions shown in Figure 8 again illustrate that the student network is able to closely approximate the uncertainty estimates produced by the teacher model. Moreover, as more number of dropout layers are inserted into the NNs for experiments with depth estimation, the relative speed-up ratio achieved by the student model is further increased due to less cached computation for the teacher. For instance, the student model achieves a speed-up ratio of 46 for the NYU V2 dataset.

4.3. Ablation Study on Additional Augmentation

To demonstrate the importance of additional augmentation during student training, we also summarize in Table 3 results when the student is trained without extra augmentation. Using extra augmentation in the student training process as discussed in Section 3.2.3 helps the student produce much better uncertainty estimation. We can also see that the

CamVid				
	ACC	IOU	ECE $(\times 10^{-3})$	AUSE $(\times 10^{-2})$
Best Single	0.900	0.641	8.27	4.46
Teacher	0.904	0.650	5.42	3.02
Student	0.909	0.653	2.96	1.91

NYU V2				
	RMSE	REL	ECE $(\times 10^{-2})$	AUSE $(\times 10^{-2})$
Best Single	0.543	0.149	70.8	6.11
Teacher	0.510	0.140	56.4	5.58
Student	0.530	0.144	56.3	5.93

Table 4: Performance of teacher and student model when a Deep Ensemble is used as the teacher. “Best Single” represents the best NN among all in the ensemble in terms of IOU/RMSE. For “Best Single”, only the aleatoric uncertainty is used to compute uncertainty metrics.

same extra augmentation does not improve the performance of the teacher’s uncertainty estimation, suggesting that the student model benefits from seeing the teacher’s predictions more closely aligned with the test-time predictive distributions, rather from data augmentation itself.

4.4. Using Deep Ensemble as the Teacher Model

To demonstrate the general applicability of the proposed algorithm, we train an ensemble of deterministic neural networks with the aleatoric uncertainty as the teacher [25]. We test the effectiveness of our method on the CamVid and the NYU V2 datasets. The training detail is identical to that described above. Due to limited computational resources, we fix the number of ensembles to five for both of the experiments. Table 4 summarises the results. The student networks significantly outperform the best single NN in the ensemble in terms of every single metric used, with better results in some of the metrics than the ensemble teacher, which consumes five times resources. Note that it can be hard for the student to learn an accurate parametric distribution with only five fixed prediction samples per pixel throughout the training. We believe the performance of the student can be further improved by using an ensemble with a larger number of individual learners as the teacher model.

5. Conclusion

We presented a two-stage teacher-student framework for fast uncertainty estimates. We conducted an extensive empirical study on two of the most common computer vision tasks. The proposed student training procedure is not only capable of producing uncertainty estimates at no extra cost but also leads to improved predictive performance and more informative uncertainty estimates. We believe the method gets us one step closer to the realm of trustworthy deep learning for computer vision.

References

- [1] Lorenzo Bertoni, Sven Kreiss, and Alexandre Alahi. Monoloco: Monocular 3d pedestrian localization and uncertainty estimation. In *Proceedings of the IEEE International Conference on Computer Vision*, pages 6861–6871, 2019.
- [2] Léonard Blier and Yann Ollivier. The description length of deep learning models. In *Advances in Neural Information Processing Systems*, pages 2216–2226, 2018.
- [3] Charles Blundell, Julien Cornebise, Koray Kavukcuoglu, and Daan Wierstra. Weight uncertainty in neural network. In *International Conference on Machine Learning*, pages 1613–1622, 2015.
- [4] Gabriel J. Brostow, Jamie Shotton, Julien Fauqueur, and Roberto Cipolla. Segmentation and recognition using structure from motion point clouds. In *ECCV (I)*, pages 44–57, 2008.
- [5] Samuel Rota Bulò, Lorenzo Porzi, and Peter Kotschieder. Dropout distillation. In *International Conference on Machine Learning*, pages 99–107, 2016.
- [6] Liang-Chieh Chen, George Papandreou, Florian Schroff, and Hartwig Adam. Rethinking atrous convolution for semantic image segmentation. *arXiv preprint arXiv:1706.05587*, 2017.
- [7] Tianqi Chen, Emily Fox, and Carlos Guestrin. Stochastic gradient hamiltonian monte carlo. In *International conference on machine learning*, pages 1683–1691, 2014.
- [8] Marius Cordts, Mohamed Omran, Sebastian Ramos, Timo Rehfeld, Markus Enzweiler, Rodrigo Benenson, Uwe Franke, Stefan Roth, and Bernt Schiele. The cityscapes dataset for semantic urban scene understanding. In *Proc. of the IEEE Conference on Computer Vision and Pattern Recognition (CVPR)*, 2016.
- [9] M. Everingham, L. Van Gool, C. K. I. Williams, J. Winn, and A. Zisserman. The PASCAL Visual Object Classes Challenge 2012 (VOC2012) Results. <http://www.pascal-network.org/challenges/VOC/voc2012/workshop/index.html>.
- [10] Di Feng, Lars Rosenbaum, and Klaus Dietmayer. Towards safe autonomous driving: Capture uncertainty in the deep neural network for lidar 3d vehicle detection. In *2018 21st International Conference on Intelligent Transportation Systems (ITSC)*, pages 3266–3273. IEEE, 2018.
- [11] Yarin Gal and Zoubin Ghahramani. Dropout as a bayesian approximation: Representing model uncertainty in deep learning. In *international conference on machine learning*, pages 1050–1059, 2016.
- [12] Yarin Gal, Riashat Islam, and Zoubin Ghahramani. Deep bayesian active learning with image data. In *Proceedings of the 34th International Conference on Machine Learning—Volume 70*, pages 1183–1192. JMLR. org, 2017.
- [13] Yonatan Geifman, Guy Uziel, and Ran El-Yaniv. Bias-reduced uncertainty estimation for deep neural classifiers. *International Conference on Learning Representations*, 2019.
- [14] Andreas Geiger, Philip Lenz, Christoph Stiller, and Raquel Urtasun. Vision meets robotics: The kitti dataset. *International Journal of Robotics Research (IJRR)*, 2013.
- [15] Wenbo Gong, Yingzhen Li, and José Miguel Hernández-Lobato. Meta-learning for stochastic gradient mcmc. *International Conference on Learning Representations*, 2019.
- [16] Chuan Guo, Geoff Pleiss, Yu Sun, and Kilian Q Weinberger. On calibration of modern neural networks. In *Proceedings of the 34th International Conference on Machine Learning—Volume 70*, pages 1321–1330. JMLR. org, 2017.
- [17] Geoffrey Hinton, Oriol Vinyals, and Jeff Dean. Distilling the knowledge in a neural network. *arXiv preprint arXiv:1503.02531*, 2015.
- [18] Gao Huang, Yixuan Li, Geoff Pleiss, Zhuang Liu, John E Hopcroft, and Kilian Q Weinberger. Snapshot ensembles: Train 1, get m for free. *arXiv preprint arXiv:1704.00109*, 2017.
- [19] Po-Yu Huang, Wan-Ting Hsu, Chun-Yueh Chiu, Ting-Fan Wu, and Min Sun. Efficient uncertainty estimation for semantic segmentation in videos. In *Proceedings of the European Conference on Computer Vision (ECCV)*, pages 520–535, 2018.
- [20] Eddy Ilg, Ozgun Cicek, Silvio Galesso, Aaron Klein, Osama Makansi, Frank Hutter, and Thomas Brox. Uncertainty estimates and multi-hypotheses networks for optical flow. In *Proceedings of the European Conference on Computer Vision (ECCV)*, pages 652–667, 2018.
- [21] Alex Kendall, Vijay Badrinarayanan, and Roberto Cipolla. Bayesian segnet: Model uncertainty in deep convolutional encoder-decoder architectures for scene understanding. *arXiv preprint arXiv:1511.02680*, 2015.
- [22] Alex Kendall and Yarin Gal. What uncertainties do we need in bayesian deep learning for computer vision? In *Advances in neural information processing systems*, pages 5574–5584, 2017.
- [23] Durk P Kingma, Tim Salimans, and Max Welling. Variational dropout and the local reparameterization trick. In *Advances in Neural Information Processing Systems*, pages 2575–2583, 2015.
- [24] Volodymyr Kuleshov, Nathan Fenner, and Stefano Ermon. Accurate uncertainties for deep learning using calibrated regression. In *International Conference on Machine Learning*, pages 2796–2804, 2018.
- [25] Balaji Lakshminarayanan, Alexander Pritzel, and Charles Blundell. Simple and scalable predictive uncertainty estimation using deep ensembles. In *Advances in Neural Information Processing Systems*, pages 6402–6413, 2017.
- [26] Christos Louizos and Max Welling. Multiplicative normalizing flows for variational bayesian neural networks. In *Proceedings of the 34th International Conference on Machine Learning—Volume 70*, pages 2218–2227. JMLR. org, 2017.
- [27] Yi-An Ma, Tianqi Chen, and Emily Fox. A complete recipe for stochastic gradient mcmc. In *Advances in Neural Information Processing Systems*, pages 2917–2925, 2015.
- [28] David JC MacKay. A practical bayesian framework for back-propagation networks. *Neural computation*, 4(3):448–472, 1992.
- [29] Wesley J Maddox, Pavel Izmailov, Timur Garipov, Dmitry P Vetrov, and Andrew Gordon Wilson. A simple baseline for bayesian uncertainty in deep learning. In *Advances in Neural Information Processing Systems*, pages 13132–13143, 2019.

- [30] Fangchang Mal and Sertac Karaman. Sparse-to-dense: Depth prediction from sparse depth samples and a single image. In *2018 IEEE International Conference on Robotics and Automation (ICRA)*, pages 1–8. IEEE, 2018.
- [31] Andrey Malinin and Mark Gales. Predictive uncertainty estimation via prior networks. In *Advances in Neural Information Processing Systems*, pages 7047–7058, 2018.
- [32] Andrey Malinin, Bruno Mlodozieniec, and Mark Gales. Ensemble distribution distillation. *arXiv preprint arXiv:1905.00076*, 2019.
- [33] Pushmeet Kohli Nathan Silberman, Derek Hoiem and Rob Fergus. Indoor segmentation and support inference from rgb-d images. *ECCV*, 2012.
- [34] Radford M Neal. *Bayesian learning for neural networks*, volume 118. Springer Science & Business Media, 2012.
- [35] Janis Postels, Francesco Ferroni, Huseyin Coskun, Nassir Navab, and Federico Tombari. Sampling-free epistemic uncertainty estimation using approximated variance propagation. In *Proceedings of the IEEE International Conference on Computer Vision*, pages 2931–2940, 2019.
- [36] Max Welling and Yee W Teh. Bayesian learning via stochastic gradient langevin dynamics. In *Proceedings of the 28th international conference on machine learning (ICML-11)*, pages 681–688, 2011.
- [37] Anqi Wu, Sebastian Nowozin, Edward Meeds, Richard E Turner, José Miguel Hernández-Lobato, and Alexander L Gaunt. Deterministic variational inference for robust bayesian neural networks. *International Conference on Learning Representations*, 2018.

6. Appendix

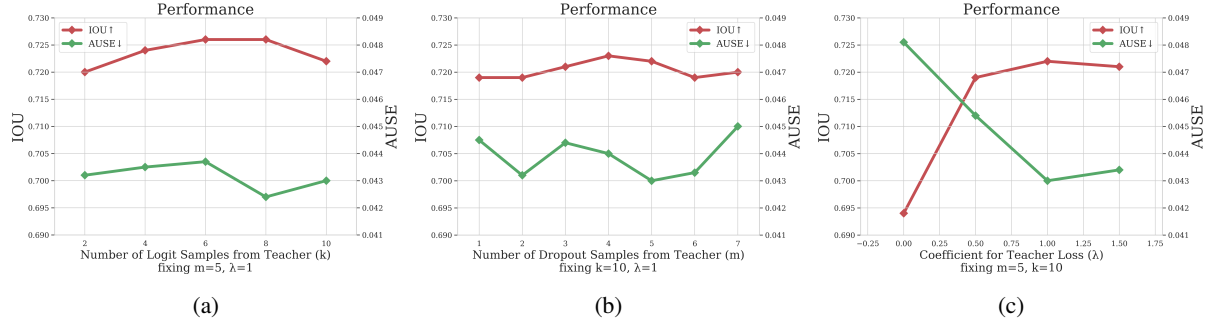


Figure 9: Ablation study conducted using the Pascal VOC2012 dataset. (a-b) Performance of the student model when the number of samples from the teacher model are varied at each mini-batch. As seen in the plots, the performance is generally insensitive to the choice of sample size. Using larger number of samples only brings slight improvement in performance up to a point. (c) Performance of student model against λ , the weight put on the teacher loss (See Eqn. 11). As seen clearly, introducing the teacher loss improves the performance of the student and the student performs the best when $\lambda = 1$.

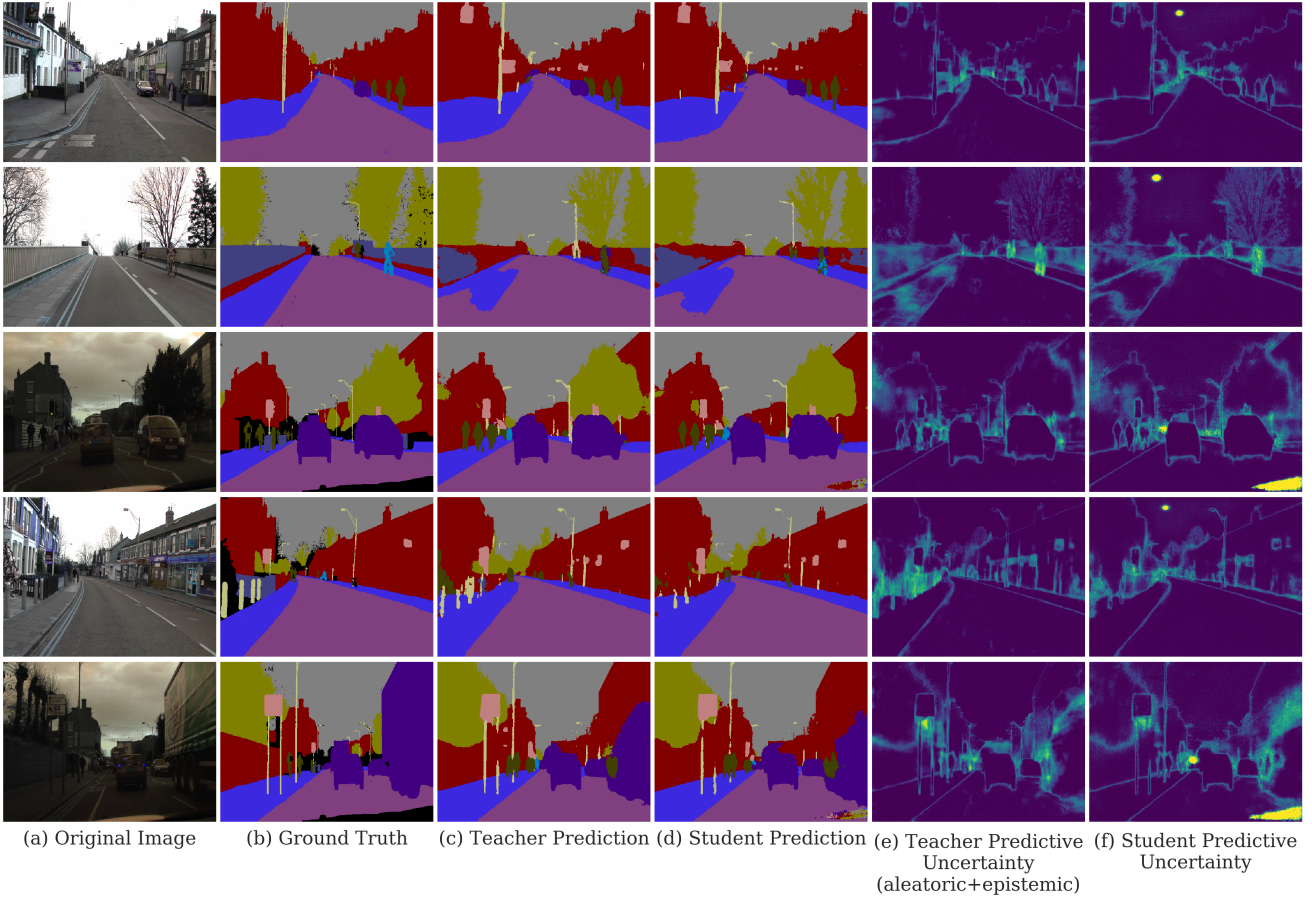


Figure 10: Additional example predictions on CamVid.

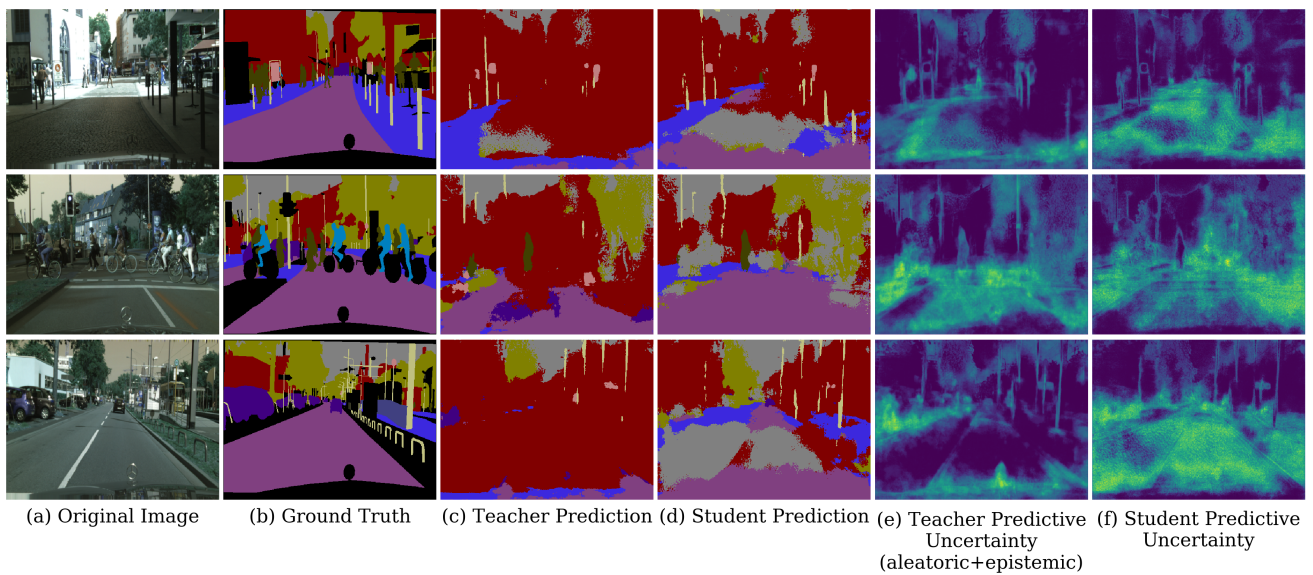


Figure 11: Example predictions on the Cityscapes dataset under distribution shift using models trained with CamVid.

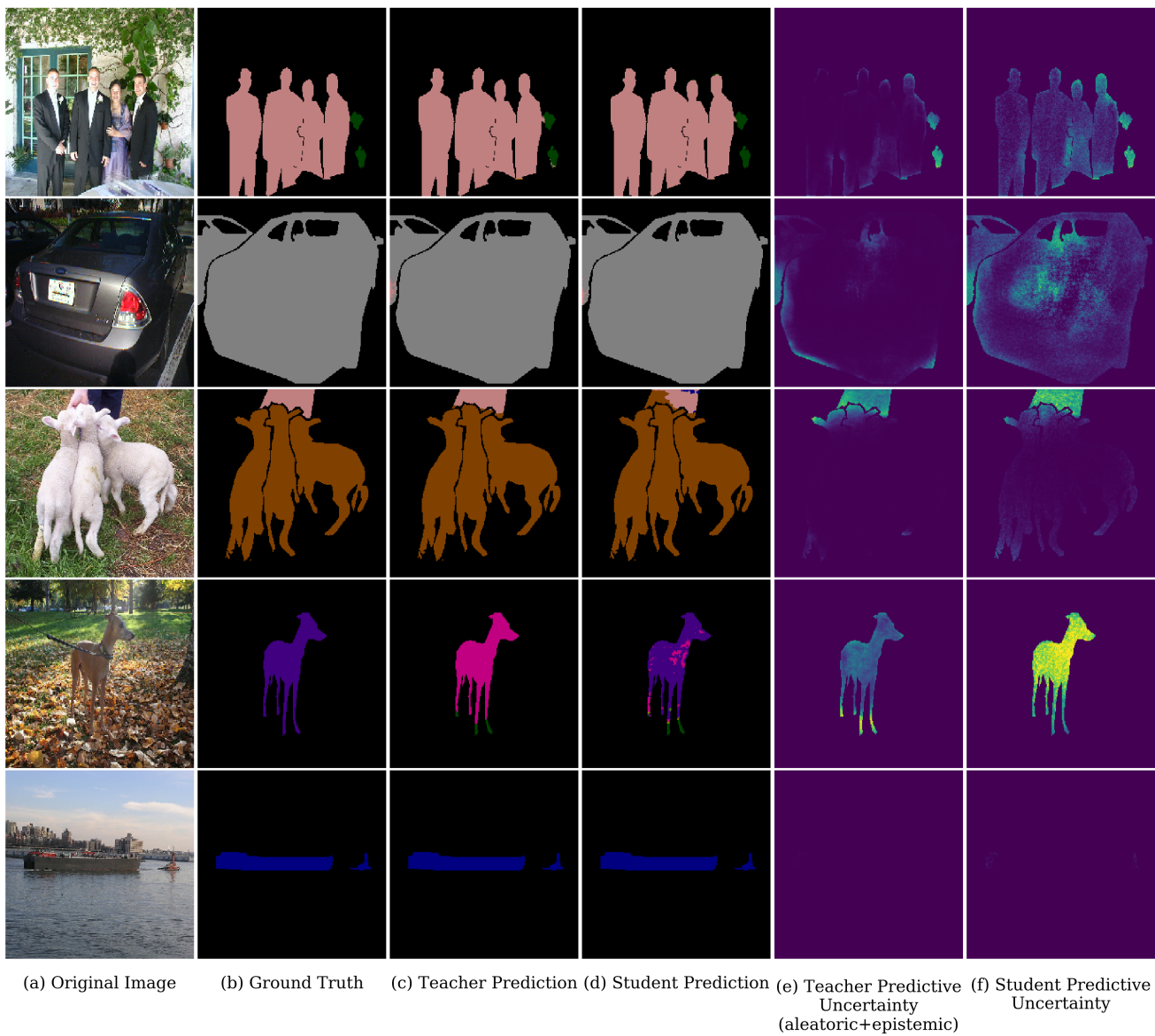


Figure 12: Additional example predictions on Pascal VOC2012.

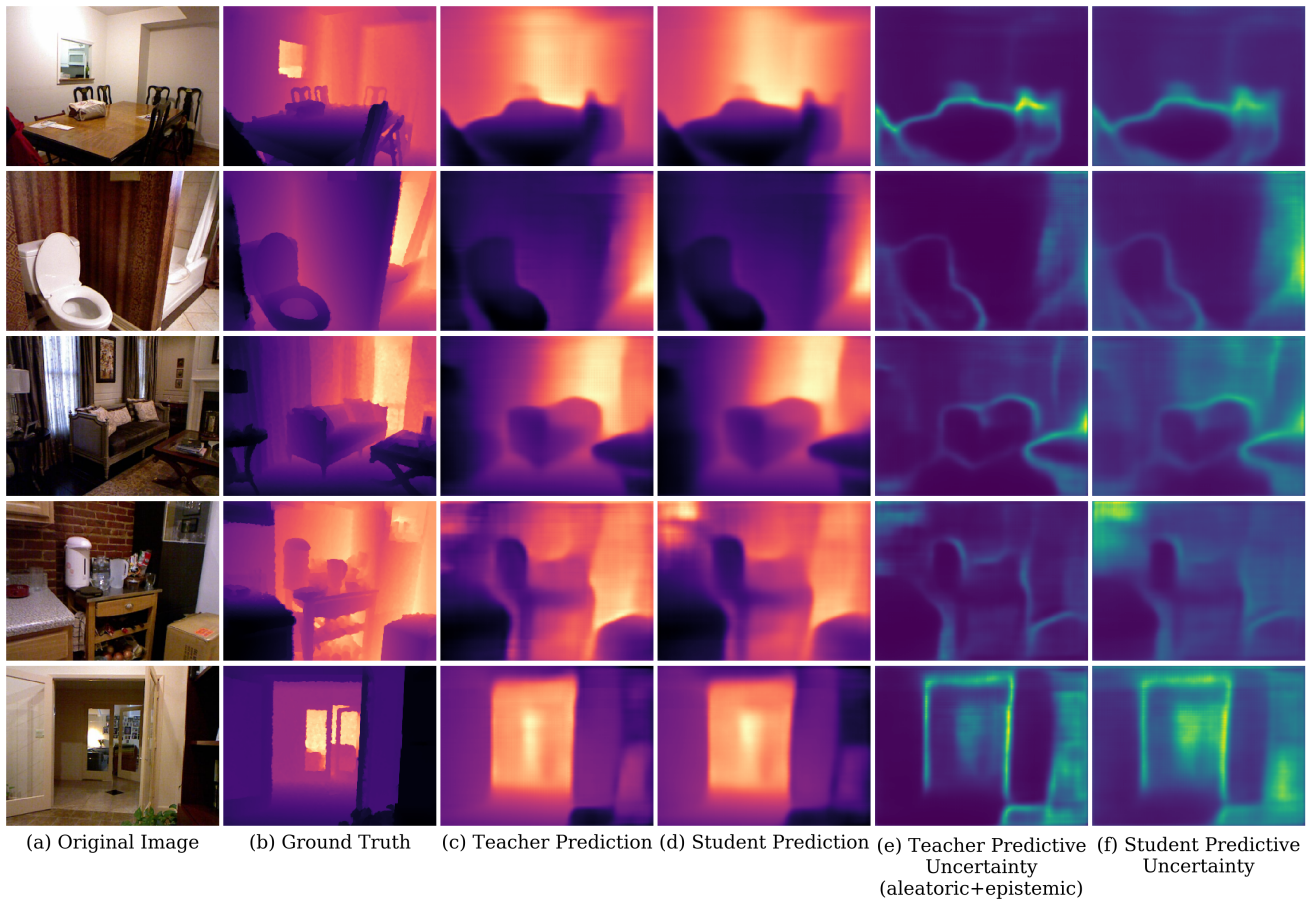


Figure 13: Additional example predictions on NYU V2.

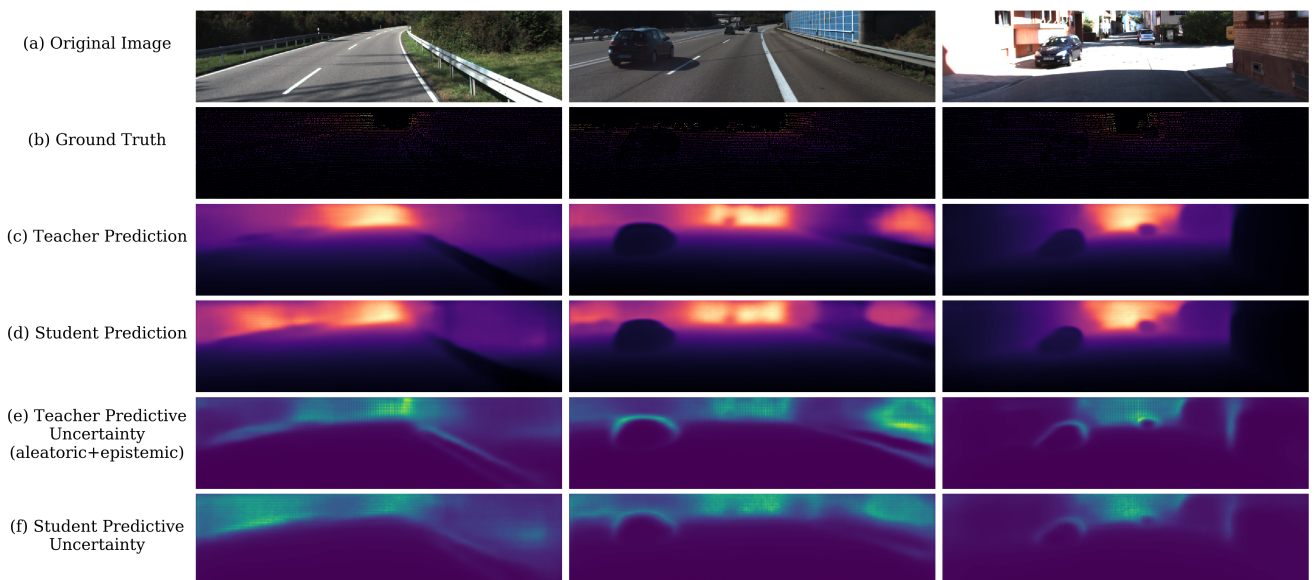


Figure 14: Example predictions on KITTI.

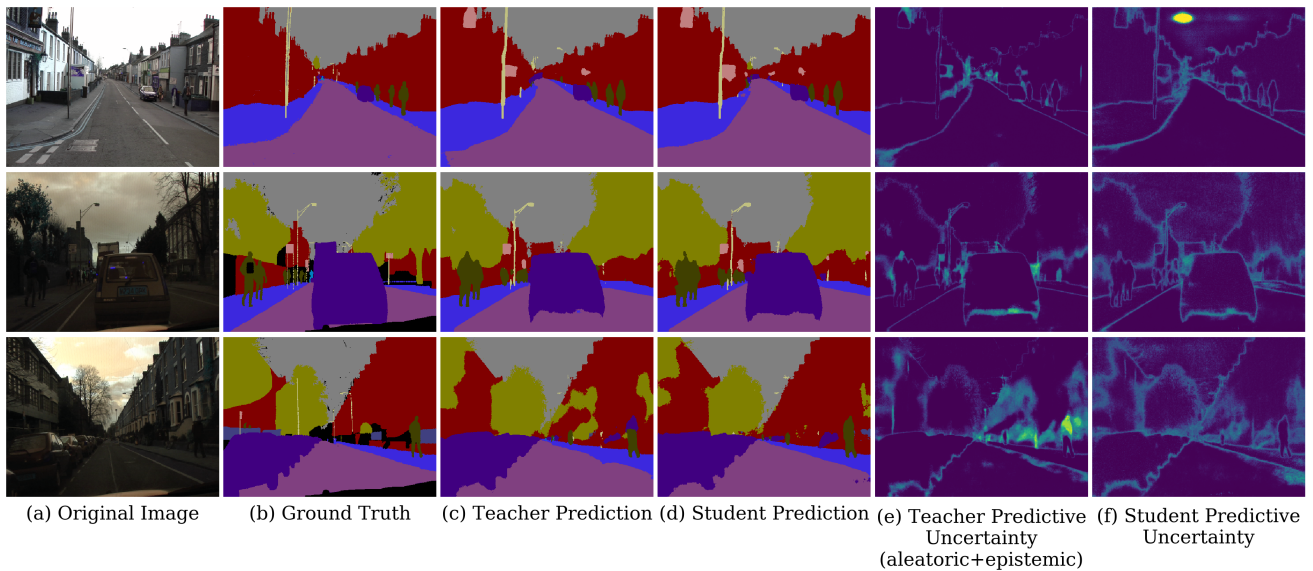


Figure 15: Example predictions on CamVid when using deep ensemble as the teacher model.

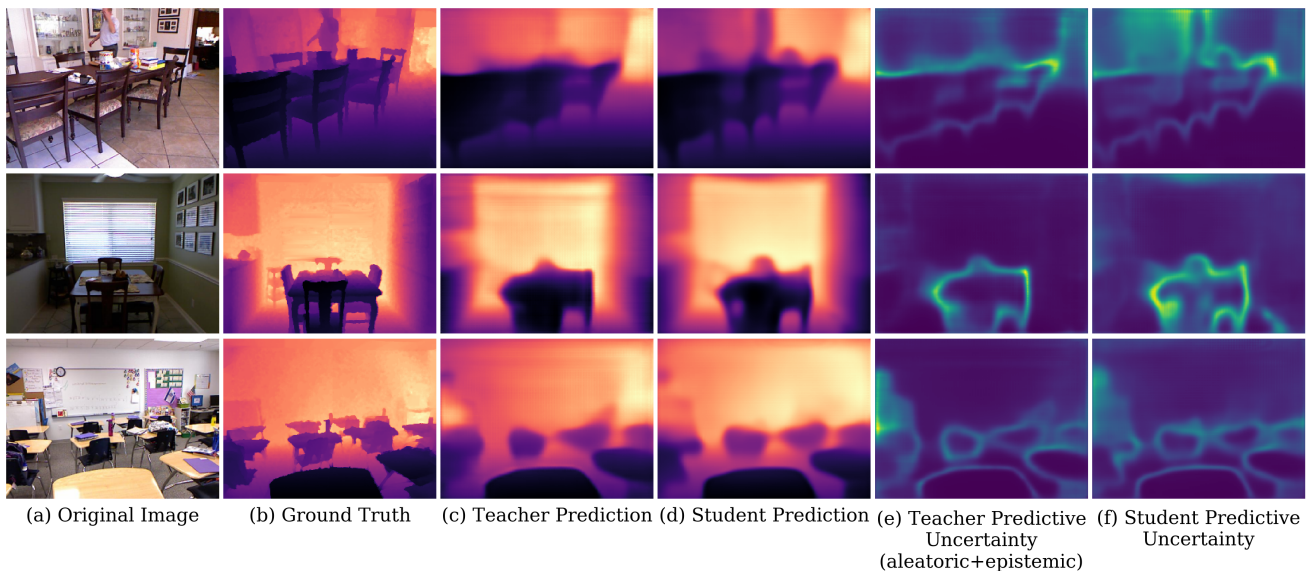


Figure 16: Example predictions on NYU V2 when using deep ensemble as the teacher model.